Symmetric and antisymmetric exchange anisotropies in quasi-one-dimensional $CuSe_2O_5$ as revealed by ESR

M. Herak,[1,2,*] A. Zorko,[1,3] D. Arčon,[1,4] A. Potočnik,[1] M. Klanjšek,[1,3] J. van Tol,[5] A. Ozarowski,[5] and H. Berger[6]

[1]*Jožef Stefan Institute, Jamova 39, SI-1000 Ljubljana, Slovenia*

[2]*Institute of Physics, Bijenička c. 46, HR-10000 Zagreb, Croatia*

[3]*EN-FIST Centre of Excellence, Dunajska 156, SI-1000 Ljubljana, Slovenia*

[4]*Faculty of Mathematics and Physics, University of Ljubljana, Jadranska 19, SI-1000 Ljubljana, Slovenia*

[5]*National High Magnetic Field Laboratory, Florida State University, Tallahassee, Florida 32310, USA*

[6]*Institute of Physics of Complex Matter, EPFL, CH-1015 Lausanne, Switzerland*

(Received 26 September 2011; revised manuscript received 7 November 2011; published 29 November 2011)

We present an electron spin resonance (ESR) study of a single-crystalline spin chain system $CuSe_2O_5$ in the frequency range between 9 and 430 GHz. In a wide temperature range above the Néel temperature $T_N = 17$ K we observe a strong and anisotropic frequency dependence of a resonance linewidth. Although a sizable interchain interaction $J_{IC} \approx 0.1J$ (J is the intrachain interaction) is present in this system, the ESR results agree well with the Oshikawa-Affleck theory for a one-dimensional $S = 1/2$ Heisenberg antiferromagnet. This theory is used to extract the anisotropies present in $CuSe_2O_5$. We find that the symmetric anisotropic exchange $J_c = (0.04 \pm 0.01)J$ and the antisymmetric Dzyaloshinskii-Moriya (DM) interaction $D = (0.05 \pm 0.01)J$ are very similar in size in this system. Staggered field susceptibility induced by the presence of the DM interaction is witnessed in the macroscopic susceptibility anisotropy.

DOI: 10.1103/PhysRevB.84.184436 PACS number(s): 75.10.Pq, 75.30.Et, 75.30.Gw, 76.30.Fc

I. INTRODUCTION

Magnetism of quasi-one-dimensional (1D) $S = 1/2$ systems is often well described by an isotropic Heisenberg Hamiltonian. Low dimensionality enhances quantum fluctuations, which in turn suppress long-range ordering. Small interchain interactions present in real systems usually stabilize long-range magnetic ordering at low, but finite, temperatures. The ground state of such systems is, however, very sensitive to the presence of small anisotropy of exchange interactions between spins, frustration, and/or defects. Depending on a local symmetry, both symmetric and antisymmetric anisotropic exchange [i.e., the Dzyaloshinskii-Moriya (DM) interaction][1] can be present. In 1D systems where the staggered g tensor and/or the staggered DM interaction is present, an applied magnetic field induces a staggered field, which opens a gap in the excitation spectrum.[2,3] Determination of the leading anisotropic terms of the spin Hamiltonian thus represents an important milestone in understanding these materials.

Magnetic resonance techniques are a very powerful tool for addressing the above points and the type of ground state in such systems.[4,5] One of the most appropriate and sensitive methods for determining the presence of small anisotropies is electron spin resonance (ESR),[6,7] since anisotropic exchange interactions broaden the otherwise exchange-narrowed ESR line.[8] Kubo-Tomita theory is a well-established method of linewidth analysis; however, it is unfortunately limited to high temperatures $T \gg J$.[9] Analysis of the ESR linewidth has evolved considerably over the last 15 years, especially regarding the $S = 1/2$ 1D Heisenberg antiferromagnet (HAF).[10–12] In case of a staggered DM interaction, its contribution to the ESR linewidth is of the same order of magnitude as the symmetric-anisotropy contribution at high temperatures,[12] despite the fact that the latter is expected to be smaller, being a higher-order perturbation correction to exchange coupling.[1] The perturbation theory calculations of the ESR line in $S = 1/2$ 1D HAFs have been extended to the entire temperature range only for the case of symmetric anisotropic exchange.[13] Relatively recently, Oshikawa and Affleck employed field-theory methods to derive a general low-temperature ESR response for half-integer-spin 1D HAFs.[10,11] Their predictions for the ESR linewidths were experimentally verified in a system with the dominant DM interaction.[14] Separately, low-temperature theories[10,11,13] were recently successfully applied to systems with symmetric anisotropic exchange.[15] However, quantitative analysis of the low-temperature ESR linewidths for the realistic systems with both anisotropies present has so far been limited.

Among the most studied 1D systems are copper oxides in which magnetism originates from Cu^{2+} ions with spin $S = 1/2$ and superexchange is usually mediated through Cu-O-Cu pathways. Copper(II) diselenium(IV) pentoxide is a new 1D copper oxide. It crystallizes in the monoclinic space group $C2/c$.[16,17] The structure consist of $S = 1/2$ Cu^{2+} chains running along the crystallographic c axis (Fig. 1). Each Se^{4+} ion carries one lone pair of electrons which plays the role of "chemical scissors".[17] The most relevant exchange interactions should be those shown in Figs. 1(a) and 1(b). The dominant intrachain interaction J is mediated through the double Cu-O-Se-O-Cu super-superexchange paths. From a phenomenological (structural) point of view, one may expect significantly smaller interchain coupling J_{IC} than J. The arrangement of the CuO_4 plaquettes and the Cu-O-Se-O-Cu bridges is such that it prevents sizable next-nearest-neighbor coupling along the chain. There are two short interchain exchange paths, but one, with the modest size of $J_{IC} \approx 0.1J$, is expected to be significantly stronger than the other [dotted lines in Fig. 1(b)].[18]

The 1D magnetic character of the system is reflected in the bulk magnetic susceptibility displaying a broad maximum at $T_{max} \approx 100$ K.[18,19] Above T_{max} it can be well modelled already in the simplest 1D Heisenberg limit, yielding the dominant intrachain exchange $J = 157$ K.[18] This value is in line with the

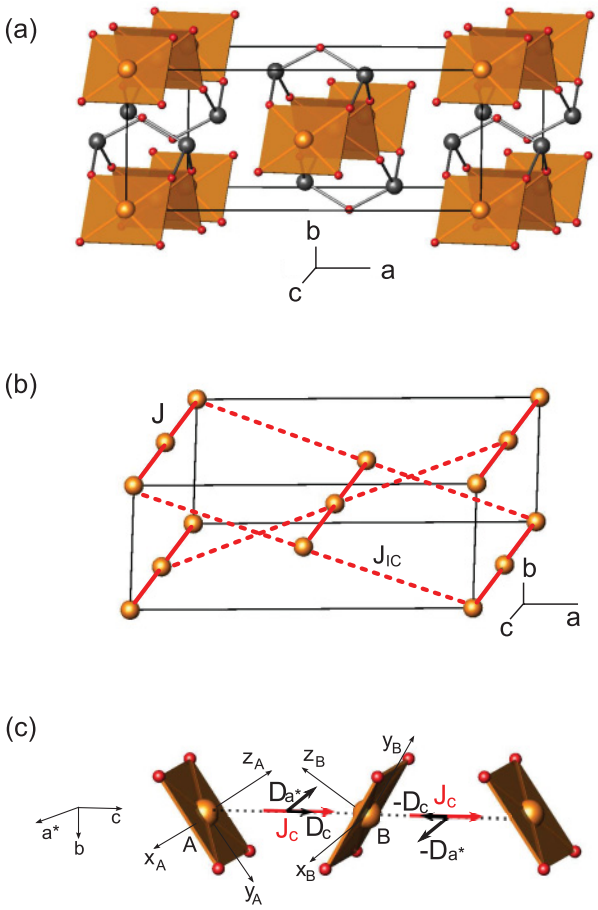

FIG. 1. (Color online) Linear-chain crystal structure in $CuSe_2O_5$. (a) Orange plaquettes represent CuO_4 rectangles and gray spheres represent Se atoms. (b) Intrachain super-superexchange path with exchange coupling J (solid lines) and dominant interchain path with exchange coupling J_{IC} (dotted lines). (c) Local coordinates of the staggered g tensor, the staggered DM vector $\mathbf{D} = (D_{a*}, 0, D_c)$, and the axis of the symmetric anisotropic exchange J_c. Dotted line represents the chain.

Curie-Weiss temperature $\Theta_{CW} = 165$ K and was also successfully theoretically accounted for by density-functional-theory (DFT) calculations, predicting $J = 165$ K and $J_{IC} = 20$ K.[18] Taking into account the interchain couplings from the DFT calculations, quantum Monte Carlo calculations could further improve the agreement between experimental susceptibility and theoretical predictions, although the disagreement below T_{max} remains noticeable, especially for the field applied along the chain direction.[18] Despite being predominantly 1D, the system orders magnetically at $T_N = 17$ K[18] due to sizable interchain interactions, as evidenced by $J_{IC} \approx T_N$. The susceptibility anisotropy below T_N is consistent with an antiferromagnetic type of spin arrangement, with spins oriented perpendicular to spin chains.[18] Raman scattering measurements showed that spin-spin correlations emerge below ≈110 K, coinciding with T_{max}, and that the system is dominated by enhanced classical spin dynamics as a consequence of a rather strong interchain interaction.[20] So far $CuSe_2O_5$ was treated as an isotropic Heisenberg spin system.[18,20] In this work we concentrate on neglected magnetic anisotropies and obtain the anisotropic spin Hamiltonian of the system by simultaneously modeling the angular, the temperature, and the frequency dependence of the ESR linewidth with the Oshikawa-Affleck theory. With the obtained anisotropy terms we significantly improve the agreement between measured and modelled susceptibility anisotropy below $T = J$. The results presented here show that both the symmetric and the antisymmetric anisotropic exchange need to be taken into account in case of $CuSe_2O_5$. In 1D cases when both types of anisotropies are present and comparable, temperature- and frequency-dependent ESR measurements are invaluable for their quantitative assessment.

II. SPIN HAMILTONIAN OF $CuSe_2O_5$

The spin Hamiltonian, which describes the spin-spin interactions in a quasi-1D spin system in the applied magnetic field $\mathbf{H}$, is

$$\mathcal{H} = \mathcal{H}_{iso} + \mathcal{H}_{ae} + \mathcal{H}_{DM} + \mathcal{H}_Z, \tag{1}$$

where

$$\mathcal{H}_{iso} = J \sum_i \mathbf{S}_i \cdot \mathbf{S}_{i+1} + J_{IC} \sum_{\langle i,j \rangle} \mathbf{S}_i \cdot \mathbf{S}_j, \tag{1a}$$

$$\mathcal{H}_{ae} = J_n \sum_i S_i^n S_{i+1}^n, \tag{1b}$$

$$\mathcal{H}_{DM} = \sum_i \mathbf{D}_i \cdot (\mathbf{S}_i \times \mathbf{S}_{i+1}), \tag{1c}$$

$$\mathcal{H}_Z = -\mu_B \sum_i \mathbf{S}_i \cdot \hat{\mathbf{g}}_i \cdot \mathbf{H}. \tag{1d}$$

$\mathcal{H}_{iso}$ is the isotropic Heisenberg interaction with intrachain exchange J and interchain exchange J_{IC} and μ_B is Bohr magneton. The first sum in $\mathcal{H}_{iso}$ runs over spins along the chain and the second over all pairs of nearest-neighboring spins $\mathbf{S}_j$ from two neighboring chains. $\mathcal{H}_{ae}$ is the symmetric anisotropic exchange with symmetry axis n and relative magnitude $\delta = J_n/J$, $\mathcal{H}_{DM}$ is the antisymmetric DM anisotropic exchange term[1] with the site-dependent DM vector $\mathbf{D}_i$ [see Fig. 1(c)]. $\mathcal{H}_Z$ is the Zeeman term where $\hat{\mathbf{g}}_i$ is the g tensor for site i.

The orientation of the anisotropic-exchange symmetry axis n may be nontrivial to determine when two or more inequivalent sites are present.[21] In $CuSe_2O_5$, the situation is further complicated by the fact that inequivalent sites A and B [Fig. 1(c)] are bridged by the nontrivial Cu-O-Se-O-Cu super-superexchange path. Nevertheless, below we show that the anisotropic exchange symmetry axis coincides with the chain direction [i.e., $n \equiv c$ in Eq. (1b); see Fig. 1(c)].

The general form of the DM vector $\mathbf{D} = (D_{a^*}, 0, D_c)$ is imposed by a twofold rotational axis along b passing through the middle of each intrachain Cu-Cu bond.[1] In addition, the symmetry of $CuSe_2O_5$ is such that the DM interaction is staggered [i.e., $\pm\mathbf{D}$; see Fig. 1(c)].

The crystal symmetry also dictates the g tensor to be staggered for A and B sites [Fig. 1(c)]. For these two sites

we thus split $\hat{\mathbf{g}}_\mathbf{i}$ in Eq. (1d) into uniform, $\hat{\mathbf{g}}_u$, and staggered, $\hat{\mathbf{g}}_s$, components and from now on use

$$\hat{\mathbf{g}}_s^{\mathrm{A,B}} = \hat{\mathbf{g}}_u \pm \hat{\mathbf{g}}_s. \tag{2}$$

III. EXPERIMENTAL

Single-crystalline $CuSe_2O_5$ samples were synthesized by the standard chemical vapor transport method, as described previously, and characterized by x-ray diffraction.[17]

The ESR experiments were performed at the X-band (9.4 GHz) and at high frequencies (HF) between 50 and 430 GHz on single-crystalline samples. The temperature dependence between 4 and 550 K was measured with a temperature stability better than ± 0.05 K. X-band measurements were performed on a home-made spectrometer equipped with a Varian TEM104 dual cavity and an Oxford Instruments ESR900 cryostat. High-frequency ESR was performed using custom-made transmission-type spectrometers at the National High Magnetic Field Laboratory (NHMFL) at Tallahassee, Florida.[22] In all cases the ESR spectra were fit to a single Lorentzian line.

Magnetic susceptibility anisotropy was determined from torque magnetometry measurements performed on a home-built torque apparatus. The resolution of the magnetometer is better than 10^{-4} dyn cm. Measurements were performed in magnetic field of 8 kOe in the temperature range 2–330 K.

IV. RESULTS

A. X-band ESR

The room-temperature angular dependence of the X-band ESR spectra (inset of Fig. 3) is shown in Fig. 2. It reveals g-factor values for the three crystallographically relevant directions, $g_{a^*} = 2.064$, $g_b = 2.140$, and $g_c = 2.226$. Taking into account the Cu-site symmetry we determine the principal eigenvalues of the g tensor: $g_x = 2.064$, $g_y = 2.089$, and $g_z = 2.277$, which are considerably higher than those previously used in theoretical calculations.[18] The principal axes of the g tensor with respect to the CuO_4 plaquettes are shown in Fig. 1(c). As expected from the crystal structure, local crystal-field symmetry at the copper site is close to being uniaxial with the local anisotropy axis pointing in the direction perpendicular to the CuO_4 plaquette (i.e., it is tilted by $\alpha = 32^\circ$ from the c axis around the a^* axis). We take into account that the total measured g tensor is in the strongly-exchanged narrowing limit given by $\hat{\mathbf{g}} = (\hat{\mathbf{g}}^{\mathrm{A}} + \hat{\mathbf{g}}^{\mathrm{B}})/2$. The uniform $\hat{\mathbf{g}}_u$ and the staggered component $\hat{\mathbf{g}}_s$ defined in Eq. (2) thus have the following form in the a^*bc frame:

$$\hat{\mathbf{g}}_u = \begin{pmatrix} 2.064 & 0 & 0 \\ 0 & 2.140 & 0 \\ 0 & 0 & 2.226 \end{pmatrix},$$

$$\hat{\mathbf{g}}_s = \begin{pmatrix} 0 & 0 & 0 \\ 0 & 0 & 0.084 \\ 0 & 0.084 & 0 \end{pmatrix}.$$

The measured g factors are temperature independent in the paramagnetic state and only slightly increase in the vicinity of T_N.

At room temperature, the ESR linewidth anisotropy is pronounced in the a^*c plane and marginal in the plane perpendicular to the chains (a^*b plane). At lower and higher temperatures, however, the anisotropy of ΔH in the a^*b plane slightly increases, as can be seen in Fig. 3. The temperature dependence of the ESR linewidth along the crystallographic directions a^*, b, and c was measured from $T_N = 17$ to 550 K (Fig. 3). Above $\approx$200 K the linewidth increases linearly with temperature for all orientations. From the value of J it is not expected that spin-spin correlations would persist up to 550 K, so we attribute this linear dependence to the phonon-assisted spin-lattice broadening.[23] We fit our high-T data to the phenomenological expression $\Delta H(T) = A + BT$ where $\Delta H^{\mathrm{ph}} = BT$ is the phonon-induced line broadening. Parameter A is the temperature-independent exchange-narrowed

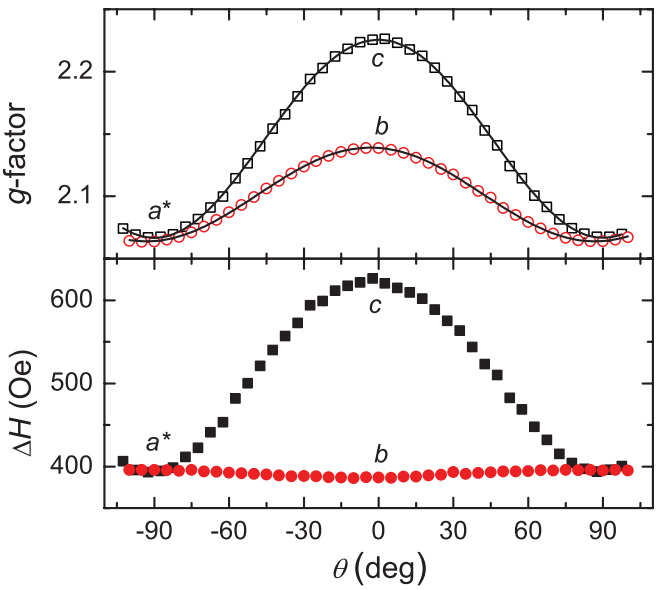

FIG. 2. (Color online) (upper panel) Angular dependence of g factor at room temperature in X-band. (lower panel) Angular dependence of linewidth at room temperature in X-band. Solid lines are fits to $g = (g_{a^*}^2 \sin^2\theta + g_{c,b}^2 \cos^2\theta)^{1/2}$.

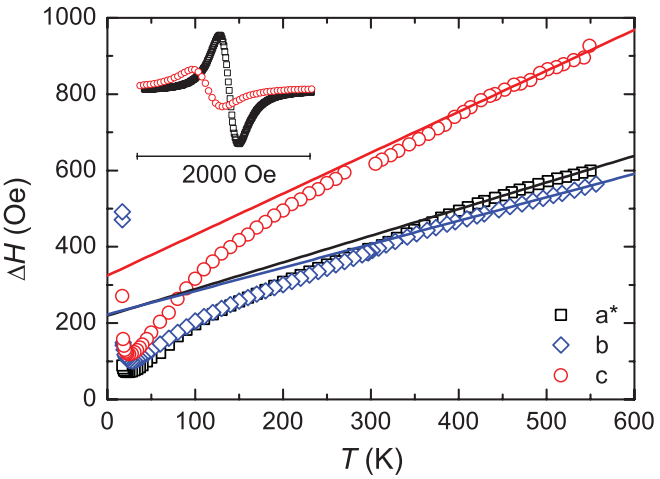

FIG. 3. (Color online) Temperature dependence of X-band ESR linewidth measured along three crystallographic directions. Solid lines represent linear fits to high-temperature data (see text). Inset shows room temperature spectra for a^* and c direction.

TABLE I. Results of linear fit $\Delta H = A + BT$ of high-temperature linewidth in 400 to 550 K range.

Direction	a^*	b	c
A (Oe)	220 ± 20	223 ± 7	313 ± 15
B (Oe/K)	0.70 ± 0.05	0.61 ± 0.01	1.10 ± 0.06

linewidth, as predicted by Kubo-Tomita theory in the $T \gg J$ regime.[9] The parameters obtained from the fits are summarized in Table I. The values of the parameters A and B depend slightly on the temperature range of the fit, which has been accounted for in the parameter errors listed in Table I.

Subtracting the phonon contribution $\Delta H^{\rm ph}$ from the raw data, ΔH results in the corrected linewidth $\Delta H^c = \Delta H - \Delta H^{\rm ph}$, which is determined by the spin-spin interactions only. At high temperatures, ΔH^c is given by the temperature-independent coefficients A (Table I) and starts to gradually decrease with decreasing temperature below room temperature. At $\approx$100 K there is a crossover to an even steeper decrease with decreasing T, which is a consequence of the evolution of spin-spin correlations below $T_{\rm max}$.[18] At $T \approx 25$ K the linewidth exhibits a minimum and then starts to sharply increase with decreasing temperature. Below T_N, the ESR spectrum disappears from the X-band. In principle, the increase of the linewidth in the vicinity of the Néel point is expected due to critical slowing down of spin fluctuations.[24] In this case the theory predicts that the linewidth becomes sensitive to the resonance frequency,[25] which was experimentally seen as a decrease of the linewidth with increasing frequency.[26] This is in contradiction with measurements in $CuSe_2O_5$, as can be seen in Fig. 4. Here, the observed linewidth increases with frequency even at temperatures well above T_N, thus suggesting some other origin of the field-dependent linewidth. Oshikawa-Affleck showed that, in 1D $S = 1/2$ HAFs, the linewidth increases with decreasing temperature for $T \ll J$ if staggered fields are present.[10,11] Since in $CuSe_2O_5$ both the staggered g tensor and the staggered DM interaction are potential sources of staggered fields, we now turn to the high-frequency ESR results. Nevertheless, we note that a large increase in the X-band linewidths below $\approx$22 K reflects the critical fluctuations in the vicinity of T_N.

B. High-frequency ESR

Temperature dependencies of the ESR linewidth measured at 240 GHz for crystal directions a^*, b, and c are shown and compared to the X-band data in insets of Fig. 4. For comparison we also show linewidth measured at 112 GHz for direction b. In contrast to the X-band data, at higher frequencies the ESR signal is observable even below $T_N = 17$ K, showing a clear anomaly in the linewidth at the transition temperature.

It is immediately clear that the magnetic field strongly affects the ESR linewidths along all crystallographic directions. By far the largest effect is seen for the magnetic field along the c direction. To quantitatively analyze the temperature and frequency (field) dependence of the linewidth we first subtracted the high-temperature phonon contribution $\Delta H^{\rm ph}$ determined at X-band frequencies. In doing so, we exploit the fact that this contribution is field-independent. The resulting

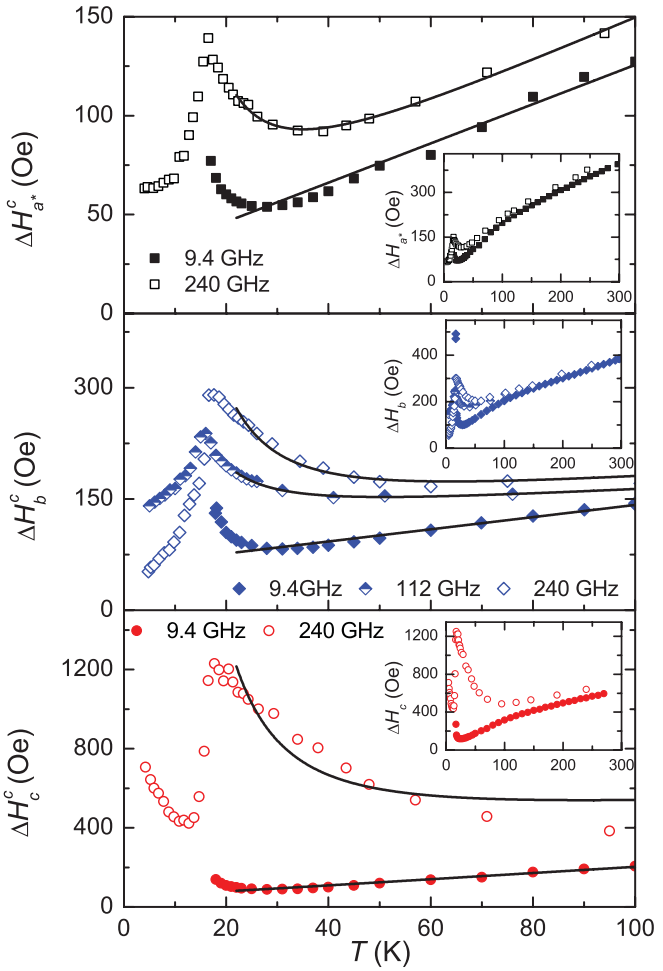

FIG. 4. (Color online) Temperature dependence of the corrected ESR linewidth ΔH^c measured at 9.4, 112, and 240 GHz for magnetic field orientations along all three crystallographic directions. Solid lines are fits to Eq. (5). Insets show temperature dependence of the raw-data linewidth measured at different frequencies.

linewidths ΔH^c, which will be discussed below, are shown in the main panels of Fig. 4.

The temperature region where the Oshikawa-Affleck theory is strictly applicable is $T_N \ll T \ll J$, although experiments have also been successfully analyzed for $T < J$.[14] In $CuSe_2O_5$, $J \approx 160$ K and the system orders antiferromagnetically at $T_N = 17$ K, so we limit our analysis to the temperature range 22 K $< T <$ 100 K. Increasing the lower limit by a few Kelvins does not influence the extracted parameters. For the Hamiltonian given by Eq. (1), the theory for the ESR linewidth in case of symmetric anisotropic exchange predicts[11,13]

$$\Delta H_{ae}(T) = \frac{2\epsilon k_B \delta^2}{g\mu_B \pi^3} T, \tag{3}$$

where $\epsilon = 2$ applies when the magnetic field is along the anisotropy n axis and $\epsilon = 1$ otherwise, k_B is the Boltzmann constant. Low-temperature logarithmic corrections can be neglected in the investigated temperature range.[11] Equation (3) predicts a linear increase of the ESR linewidth with T, which is exactly what we observe for ΔH^c for all three directions and $T \gg 25$ K (Fig. 4). Thus we conclude that the symmetric anisotropic exchange is present in $CuSe_2O_5$.

Clear deviations from the linear temperature dependence of ΔH^c in the low-temperature region imply that the staggered field is also present. Its contribution to the linewidth is given by[10,11]

$$\Delta H_{sf}(H,T) = 0.69 g\mu_B \frac{k_B J}{(k_B T)^2} h_s^2 \sqrt{\ln\left(\frac{J}{T}\right)}, \qquad (4)$$

where the staggered field $h_s = c_s H$ is proportional to the applied field H and the anisotropic staggered field coefficient c_s.

Since there are no cross terms between the symmetric and the antisymmetric anisotropic exchange, the total ESR linewidth for 1D systems described by Hamiltonian (1) is given by

$$\Delta H(H,T) = \Delta H_0 + \Delta H_{ae}(T) + \Delta H_{sf}(H,T). \qquad (5)$$

ΔH_0 is the temperature-independent linewidth in the high-T limit, which—according to Refs. 10 and 11 —contains both the field-independent and the field-dependent contributions.

Simultaneous fitting of both the temperature (Fig. 4) and the frequency dependence (Fig. 5) of ΔH^c to the model given by Eq. (5) allows us to obtain parameters ΔH_0, δ and staggered field coefficients $c_{s,i}$ for all three magnetic field orientations. The details of the more involved analysis of the frequency dependence are given in Appendix A. Both linewidth dependencies can be fit (Figs. 4 and 5) with the single set of parameters: $c_{s,a^*} = 0.009 \pm 0.004$, $c_{s,b} = 0.021 \pm 0.004$, $c_{s,c} = 0.062 \pm 0.006$, $\delta = 0.04 \pm 0.01$. Simulations also yield that the c axis is the symmetric-anisotropy axis; namely $n = c$ in the Hamiltonian (1b). Worse agreement is found for X-band data below ≈25 K, which we attribute to the vicinity of the phase transition overshadowing the effect of the induced staggered field. To affirm the correctness of the above fitting parameters, we now turn to the low-temperature angular dependence of the linewidth at high frequencies.

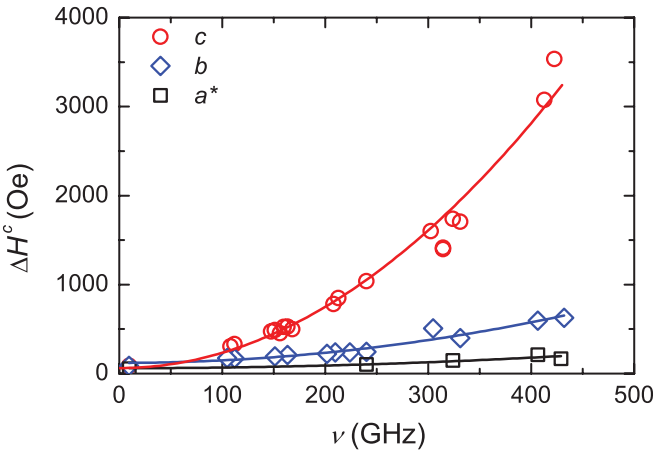

FIG. 5. (Color online) Frequency dependence of the corrected ESR linewidth ΔH^c at $T = 25$ K. Solid lines are fits to Eq. (A1).

V. STAGGERED FIELD ANALYSIS AND DM VECTOR

In $CuSe_2O_5$, the crystal structure implies that both the staggered g tensor and the staggered DM vector are present, giving the staggered field

$$\mathbf{h}_s = \hat{\mathbf{g}}_u^{-1}\left(\hat{\mathbf{g}}_s + \frac{1}{2J}\mathbf{D}\times\hat{\mathbf{g}}_u\right)\cdot\mathbf{H}. \qquad (6)$$

The staggered field contribution to the ESR linewidth is determined by the magnitude of $\mathbf{h}_s$, which is proportional to the staggered field coefficients c_s. For the cases when magnetic field is aligned along the three crystallographic axes, in $CuSe_2O_5$ the staggered field coefficients have the following form:

$$\begin{aligned} c_{s,a^*} &= \frac{|D_c| g_{a^*}}{2g_b}, \\ c_{s,b} &= \sqrt{\left(\frac{D_c g_b}{2g_{a^*}}\right)^2 + \left(\frac{D_{a^*} g_b + 2g_{bc}}{2g_c}\right)^2}, \\ c_{s,c} &= \left|\frac{2g_{bc} - D_{a^*} g_c}{2g_b}\right|. \end{aligned} \qquad (7)$$

The general expression for c_s for arbitrary direction of magnetic field can be found in Appendix B.

Using the experimentally determined g tensor [Eq. (3)] and values of $c_{s,i}$, we can now also obtain the DM vector from Eqs. (7). Solving equations for c_{s,a^*} and $c_{s,b}$ for $\mathbf{D}$ gives four possible solutions: $\mathbf{D}_1^{\pm} = (-0.114 \pm 0.015,\ 0,\ \pm 0.024 \pm 0.014)J$ and $\mathbf{D}_2^{\pm} = (-0.043 \pm 0.015,\ 0,\ \pm 0.024 \pm 0.014)J$. Alternatively, solving equations for $c_{s,c}$ and $c_{s,b}$ gives two real values: $\mathbf{D}_3^{\pm} = (-0.045 \pm 0.011,\ 0,\ \pm 0.027 \pm 0.014)J$. Since DM vectors $\mathbf{D}_2^{\pm}$ and $\mathbf{D}_3^{\pm}$ nearly coincide, we take this solution as the correct DM vector.

Finally, we note that the average of $\mathbf{D}_2^{\pm}$ and $\mathbf{D}_3^{\pm}$ [i.e., the DM vector $\mathbf{D} = (-0.044 \pm 0.010,\ 0,\ \pm 0.0255 \pm 0.010)J$] also accounts for the angular dependence of the linewidth measured at 240 GHz and 25 K (Fig. 6). Unfortunately, the present data do not allow us to also determine the sign of the c component of $\mathbf{D}$ because the calculated linewidth for both cases describes the data equally well.

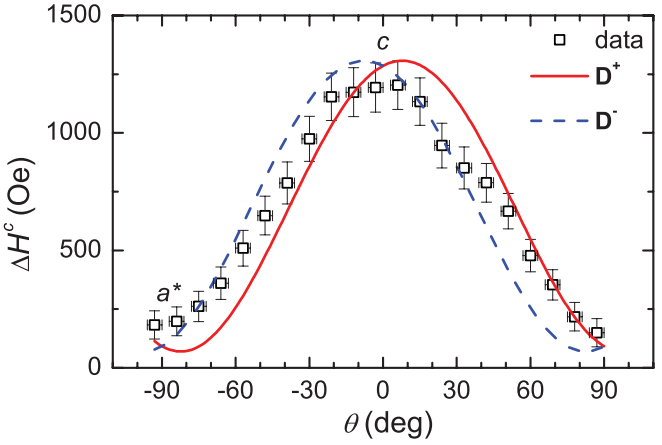

FIG. 6. (Color online) Angular dependence of ESR linewidth measured at 240 GHz and 25 K in the a^*c plane. Solid and dotted lines are calculated linewidths using Eq. (5) and $\mathbf{D}^+ = (-0.044,\ 0,\ +0.0255)J$ and $\mathbf{D}^- = (-0.044,\ 0,\ -0.0255)J$, respectively. In both cases $\delta = 0.04$. See text for details.

VI. DISCUSSION AND CONCLUSIONS

The main experimental finding of this work is the determination of anisotropies in the 1D HAF $CuSe_2O_5$. Both anisotropies, the symmetric anisotropic exchange, and the antisymmetric DM interaction are sizable and comparable. The former anisotropy is expected to open a gap in the excitation spectrum already in zero magnetic field. This gap is expected to decrease with increasing field.[27] However, in contrast, at high magnetic fields the staggered field contribution will dominate and define the energy gap. In this limit, the excitation gap is expected to scale with magnetic field, similarly as in other prototypical 1D HAF systems like Cu-benzoate[2,28] or Cu-pyrimidine dinitrate.[29,30] The crossover between the two regimes has to be addressed in the future from both the theoretical as well as the experimental point of view, since it may lead to unconventional static and dynamic magnetic properties.

The presence of both anisotropies should explain the unresolved issue of poor fitting of magnetic susceptibility below $T_{\max}$.[18] Staggered magnetic anisotropy is responsible for the additional anisotropy in the magnetic susceptibility for $T < J$. For this reason we measured the temperature dependence of the magnetic susceptibility anisotropy $\Delta\chi_{ba^*} = \chi_b - \chi_{a^*}$ and $\Delta\chi_{ca^*} = \chi_c - \chi_{a^*}$ by means of torque magnetometry (Fig. 7). The measured magnetic susceptibility anisotropies clearly cannot be explained with the simple 1D HAF Bonner-Fisher susceptibility[31,32] (Fig. 7). In the calculations we used $J = 161$ K, while interchain interactions with $J_{\mathrm{IC}} = 0.1J$ and the number of nearest-neighbor chains $z = 2$ have been taken into account in the mean-field approximation.[32] The quality of the fit significantly improves when staggered susceptibility $\chi_{s,i}(T)$ is taken into account. $\chi_{s,i}(T)$ is expressed as[2,3]

$$\chi_{s,i}(T) = 0.278c_{s,i}^2 \left(\frac{N_A g^2 \mu_B^2}{4k_B}\right) \frac{\sqrt{\ln(J/T)}}{T} \tag{8}$$

where i represents the direction of the applied magnetic field. Using above given staggered susceptibility we expand a quantitative agreement with susceptibility anisotropy data down to 50 K with somewhat increased staggered field parameters, $c_{s,a^*} = 0.024$, $c_{s,b} = 0.047$ and $c_{s,c} = 0.13$, the discrepancy between the staggered field parameters obtained from ESR and from susceptibility being similar to what was observed for Cu benzoate.[3] Thus determined magnetic anisotropies even manage to describe the plateau in $\Delta\chi_{ca^*}$ below $T_{\max}$ as well as mimic the sudden upturn in $\Delta\chi_{ba^*}$ below 50 K.

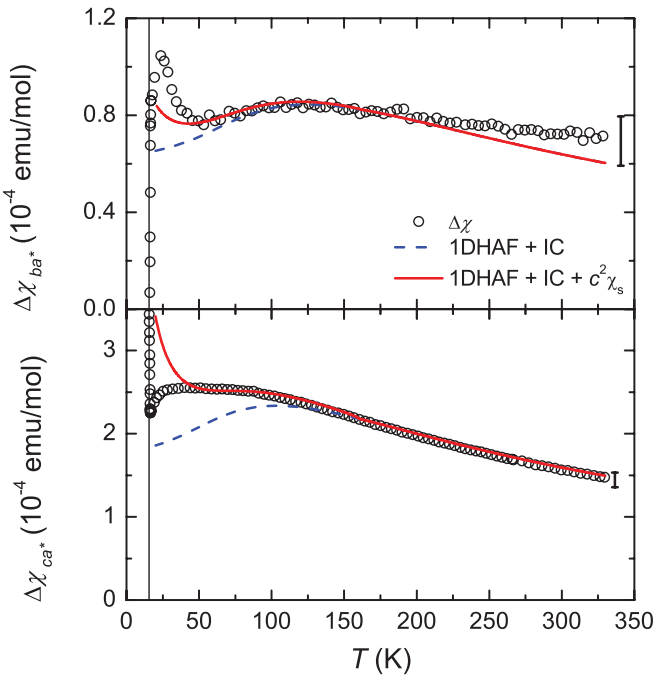

FIG. 7. (Color online) Susceptibility anisotropy measured in the a^*b plane (upper panel) and a^*c plane (lower panel). Lines represent comparison between susceptibility anisotropy obtained from 1D HAF with interchain interactions (dotted lines) and when staggered susceptibility is included (solid lines). See text for details. The error bar is shown on the right of the data. The vertical line represents the ordering temperature T_N.

In conclusion, we studied a quasi-one-dimensional HAF $CuSe_2O_5$ with temperature-, frequency-, and angular-dependent ESR. ESR linewidth analysis within the OA theory for $S = 1/2$ 1D HAFs allowed us to obtain the values of symmetric anisotropic exchange interaction $J_c = (0.04 \pm 0.01)J$ and antisymmetric DM interaction $|\mathbf{D}| = (0.05 \pm 0.01)J$. $CuSe_2O_5$ thus appears to be an extremely interesting system where both anisotropies are of similar strength, which has some profound effects on the ground-state and magnetic susceptibility anisotropies. Present results thus challenge detailed investigations of the low-energy excitation spectrum and the staggered spin susceptibilities by inelastic neutron diffraction or local probe nuclear magnetic resonance techniques. Finally, we stress that this work also demonstrates how to systematically approach ESR data when both anisotropies are present in the 1D system.

ACKNOWLEDGMENTS

M. H. acknowledges financial support by the Slovene Human Resources Development and Scholarship fund under grant No. 11013-57/2010-5, Postdoc program of the Croatian Science Foundation (Grant No. O-191-2011), and the resources of the Croatian Ministry of Science, Education and Sports under Grant No. 035-0352843-2846. A. Z. and D. A. acknowledge the financial support of the Slovenian Research Agency (projects J1-2118 and BI-US/09-12-040).

APPENDIX A: FREQUENCY DEPENDENCE OF LINEWIDTH AT $T = 25$ K

Frequency dependence of the linewidth measured at 25 K for all three crystallographic directions is shown in Fig. 5. To fit the data to the Eq. (5), we need to resolve Eq. (5) into the frequency-dependent and frequency-independent contributions. The frequency-dependent contributions are expected to depend on ν^2, so we fit our data for given direction i to

$$\Delta H_i(T,\nu) = \alpha_i(T) + \beta_i(T)\nu^2, \quad i = a^*, b, c, \tag{A1}$$

where

$$\alpha_i(T) = \Delta H_{0,i}(\nu = 0) + \Delta H_{ae,i}(T), \tag{A1a}$$

$$\beta_i(T)\nu^2 = \Delta H_{0,i}(\nu) + \Delta H_{sf,i}(\nu, T). \tag{A1b}$$

TABLE II. Results of fit of frequency dependence of linewidth at $T = 25$ K (shown in Fig. 5) to Eq. (A1).

	α (Oe)	β (10^{-3} Oe/GHz^2)	ΔH_0 (240 GHz) (Oe)	c_s
a^*	60 ± 20	0.7 ± 0.2	20 ± 5	0.010 ± 0.002
b	120 ± 18	2.9 ± 0.2	20 ± 5	0.026 ± 0.001
c	62 ± 61	17.3 ± 0.8	90 ± 5	0.068 ± 0.002

The temperature-independent part ΔH_0 in Eq. (5) is also split in two parts: the frequency-independent $\Delta H_{0,i}(\nu = 0)$ and the frequency-dependent $\Delta H_{0,i}(\nu)$. Our intention is to obtain the parameters δ and c_s. However, both parameters α and β obtained from the fit consist of two unknown parts. The difficulty arises from the fact that both $\Delta H_{0,i}(\nu = 0)$ and $\Delta H_{0,i}(\nu)$ need to be determined first. The origin of these contributions was discussed by Oshikawa-Affleck.[11] From their analysis, $\Delta H_{0,i}(\nu = 0)$ is expected to be negligibly small because it is proportional to D^4/J^3. If we neglect it, we obtain $\delta = 0.03$, which is in good agreement with $\delta = 0.04 \pm 0.01$ obtained from fits of temperature dependence of the linewidth. To determine the frequency-dependent high-T term $\Delta H_{0,i}(\nu)$, we assume that the 9 GHz data are the zero-frequency linewidth limit and subtract it from the 240 GHz linewidth to obtain the frequency-dependent part, $\Delta H_0(\nu = 240$ GHz). From Eq. (A1b) we see that, by subtracting this from $\beta_i(25$ K) (240 GHz)^2 we obtain $\Delta H_{sf}(\nu = 240\,\text{GHz},\ 25\,\text{K})$. Once $\Delta H_{sf}(\nu = 240\,\text{GHz},\ 25\,\text{K})$ is obtained, the staggered field coefficients can be calculated by using Eq. (4). The results are summarized in Table II and correspond, within errors, to the ones obtained from the fits of the temperature dependence of the linewidth.

APPENDIX B: ANGULAR DEPENDENCE OF LINEWIDTH AT $T = 25$ K AND $\nu = 240$ GHZ

Assuming the most general staggered DM vector allowed by symmetry, $\mathbf{D} = (D_{a^*},0,D_c)J$, the following expression is obtained for the staggered field coefficient c_s from Eq. (6):

$$c_s^2(\theta,\varphi) = \left(\frac{D_c g_b \sin\theta \sin\varphi}{2g_{a^*}}\right)^2 + \left(\frac{(2g_{bc} - D_{a^*} g_c)\cos\theta + D_c g_{a^*} \cos\varphi \sin\theta}{2g_b}\right)^2 + \left(\frac{(D_{a^*} g_b + 2g_{bc})\sin\theta \sin\varphi}{2g_c}\right)^2. \quad \text{(B1)}$$

g-tensor components can be directly read from Eq. (3), θ is the polar angle and φ is the azimuthal angle (we take $x = a^*$, $y = b$, and $z = c$). Equation (B1) gives the coefficient c_s for some general direction of the applied field. Experimentally determined staggered field coefficients (Sec. IV B) are equated with Eq. (B1) in the following way: $c_{s,a^*} = c_s(\theta = \pi/2, \varphi = 0)$, $c_{s,b} = c_s(\theta = \pi/2, \varphi = \pi/2)$, and $c_{s,c} = c_s(\theta = 0)$, which gives the result (7) quoted in the main text.

Measured angular dependence of the linewidth shown in Fig. 6 can be compared to Eq. (5) without any free parameters using expression (B1) for the staggered field parameter by setting $\varphi = 0$. We assume the following angular dependence of parameter ϵ in Eq. (3): $\epsilon = 1 + \cos^2\theta$ which gives $\epsilon = 1$ for a^* direction and $\epsilon = 2$ for c, in accord with the previously obtained results. The temperature-independent correction ΔH_0 in Eq. (5) is also angular dependent. We simulate this dependence in the following way: $\Delta H_0(\theta) = \Delta H_{0,a^*} + (\Delta H_{0,c} - \Delta H_{0,a^*})\cos^2\theta$, where $\Delta H_{0,a^*} = 40$ Oe and $\Delta H_{0,c} = 450$ Oe are the temperature-independent corrections obtained from fits of Eq. (5) to the temperature dependence of the linewidth along the a^* and c axes, respectively. We also take $\delta = 0.04$ obtained from the same fits, and $\mathbf{D}^{\pm} = (-0.044, 0, \pm 0.0255)J$.

*mirta.herak@ijs.si

[1] T. Moriya, Phys. Rev. Lett. **4**, 228 (1960); Phys. Rev. **120**, 91 (1960).

[2] M. Oshikawa and I. Affleck, Phys. Rev. Lett. **79**, 2883 (1997).

[3] I. Affleck and M. Oshikawa, Phys. Rev. B **60**, 1038 (1999); **62**, 9200 (2000).

[4] H.-A. K. von Nidda, N. Büttgen, and A. Loidl, Eur. Phys. J. - Special Topics **180**, 161 (2010).

[5] K. Katsumata, J. Phys. Condens. Matter **12**, R589 (2000).

[6] A. Zorko, S. Nellutla, J. van Tol, L. C. Brunel, F. Bert, F. Duc, J.-C. Trombe, M. A. de Vries, A. Harrison, and P. Mendels, Phys. Rev. Lett. **101**, 026405 (2008).

[7] A. Zorko, D. Arčon, H. van Tol, L. C. Brunel, and H. Kageyama, Phys. Rev. B **69**, 174420 (2004).

[8] A. Abragam and B. Bleaney, *Electron Paramagnetic Resonance of Transition Ions* (Oxford University Press, Oxford, 1970).

[9] R. Kubo and K. Tomita, J. Phys. Soc. Jpn. **9**, 888 (1954).

[10] M. Oshikawa and I. Affleck, Phys. Rev. Lett. **82**, 5136 (1999).

[11] M. Oshikawa and I. Affleck, Phys. Rev. B **65**, 134410 (2002); **76**, 109901 (2007).

[12] J. Choukroun, J.-L. Richard, and A. Stepanov, Phys. Rev. Lett. **87**, 127207 (2001).

[13] Y. Maeda, K. Sakai, and M. Oshikawa, Phys. Rev. Lett. **95**, 037602 (2005).

[14] S. A. Zvyagin, A. K. Kolezhuk, J. Krzystek, and R. Feyerherm, Phys. Rev. Lett. **95**, 017207 (2005).

[15] B. Náfrádi, A. Olariu, L. Forró, C. Mézière, P. Batail, and A. Jánossy, Phys. Rev. B **81**, 224438 (2010).

[16] P. G. Meunier, C. Svensson, and A. Carpy, Acta Crystallogr. Sect. B **32**, 2664 (1976).

[17] R. Becker and H. Berger, Acta Crystallogr. Sect. E **62**, i256 (2006).

[18] O. Janson, W. Schnelle, M. Schmidt, Y. Prots, S.-L. Drechsler, S. K. Filatov, and H. Rosner, New J. Phys. **11**, 113034 (2009).

[19] O. Kahn, M. Verdaguer, J. J. Girerd, J. Galy, and F. Maury, Solid State Commun. **34**, 971 (1980).

[20] K.-Y. Choi, P. Lemmens, and H. Berger, Phys. Rev. B **83**, 174413 (2011).

[21] R. M. Eremina, M. V. Eremin, V. N. Glazkov, H.-A. Krug von Nidda, and A. Loidl, Phys. Rev. B **68**, 014417 (2003).

[22] A. K. Hassan, L. A. Pardi, J. Krzystek, A. Sienkiewicz, P. Goy, M. Rohrer, and L. C. Brunel, J. Magn. Reson. **142**, 300 (2000).
[23] M. S. Seehra and T. G. Castner, Phys. Kondens. Mater. **7**, 185 (1968).
[24] D. L. Huber, Phys. Rev. B **6**, 3180 (1972).
[25] K. Kawasaki, Prog. Theor. Phys. **39**, 285 (1968).
[26] M. S. Seehra, J. Appl. Phys. **42**, 1290 (1971).
[27] S. Kimura, H. Yashiro, K. Okunishi, M. Hagiwara, Z. He, K. Kindo, T. Taniyama, and M. Itoh, Phys. Rev. Lett. **99**, 087602 (2007).
[28] D. C. Dender, P. R. Hammar, D. H. Reich, C. Broholm, and G. Aeppli, Phys. Rev. Lett. **79**, 1750 (1997).
[29] R. Feyerherm, S. Abens, D. Günther, T. Ishida, M. Meißner, M. Meschke, T. Nogami, and M. Steiner, J. Phys. Condens. Matter **12**, 8495 (2000).
[30] S. A. Zvyagin, A. K. Kolezhuk, J. Krzystek, and R. Feyerherm, Phys. Rev. Lett. **93**, 027201 (2004).
[31] J. C. Bonner and M. E. Fischer, Phys. Rev. **135**, A640 (1964).
[32] D. C. Johnston, R. K. Kremer, M. Troyer, X. Wang, A. Klümper, S. L. Bud'ko, A. F. Panchula, and P. C. Canfield, Phys. Rev. B **61**, 9558 (2000).